Universidad Continental

FACULTAD DE INGENIERÍA

Escuela Académico Profesional de Ingeniería Civil

Tesis

Influence of Axial Load on the Ductility of Type "C" Reinforced Concrete Walls with Longitudinal Reinforcement Variation in the Cores

Meyer David Hilario Martel
Jhon Josue Canchanya Taipe
Janela Azucena Condor Gonzalez
Johan James Hinostroza Yucra

Para optar el Título Profesional de
Ingeniero Civil

Huancayo, 2025

Universidad Continental

INFORME DE CONFORMIDAD DE ORIGINALIDAD DE TRABAJO DE INVESTIGACIÓN

A	:	Decano de la Facultad de Ingeniería
DE	:	Manuel Ismael Laurencio Luna Asesor de trabajo de investigación
ASUNTO	:	Remito resultado de evaluación de originalidad de trabajo de investigación
FECHA	:	6 de Enero de 2025

Con sumo agrado me dirijo a vuestro despacho para informar que, en mi condición de asesor del trabajo de investigación:

Título:
Influence of Axial Load on the Ductility of Type "C" Reinforced Concrete Walls with Longitudinal Reinforcement Variation in the Cores.

URL / DOI:
https://doi.org/10.1007/978-981-99-6368-3_22

Autores:
1. Meyer David Hilario Martel – EAP. Ingeniería Civil
2. Jhon Josue Canchanya Taipe – EAP. Ingeniería Civil
3. Janela Azucena Condor Gonzalez – EAP. Ingeniería Civil
4. Johan James Hinostroza Yucra – EAP. Ingeniería Civil

Se procedió con la carga del documento a la plataforma "Turnitin" y se realizó la verificación completa de las coincidencias resaltadas por el software dando por resultado 4 % de similitud sin encontrarse hallazgos relacionados a plagio. Se utilizaron los siguientes filtros:

- Filtro de exclusión de bibliografía — SI [x] NO [ ]
- Filtro de exclusión de grupos de palabras menores — SI [ ] NO [x]
  Nº de palabras excluidas **(en caso de elegir "SI"):**
- Exclusión de fuente por trabajo anterior del mismo estudiante — SI [x] NO [ ]

En consecuencia, se determina que el trabajo de investigación constituye un documento original al presentar similitud de otros autores (citas) por debajo del porcentaje establecido por la Universidad Continental.

Recae toda responsabilidad del contenido del trabajo de investigación sobre el autor y asesor, en concordancia a los principios expresados en el Reglamento del Registro Nacional de Trabajos conducentes a Grados y Títulos – RENATI y en la normativa de la Universidad Continental.

Atentamente,

Influence of Axial Load on the Ductility of Type "C" Reinforced Concrete Walls with Longitudinal Reinforcement Variation in the Cores

Meyer David Hilario Martel, Jhon Josue Canchanya Taipe, Janela Azucena Condor Gonzalez, and Johan James Hinostroza Yucra

Abstract Type "C" shear walls are structural elements with a great capacity to absorb seismic forces that are commonly used in elevator boxes. The present research aims to show the effect of the axial load from 980.6 to 7844.8 KN on the ductility of the walls called (M1) and (M2), also evaluating the ductility in relation to variation of reinforcement longitudinal in the cores, for which trilinear diagrams of moment–curvature of both walls were generated. The results showed that the increase in axial load is inversely proportional to the ductility of the wall. On the other hand, the increase in axial load is directly proportional to the values of moments at each point of the moment–curvature diagram, but inversely proportional to the curvature at the points of the yield of steel and exhaustion of the maximum capacity. The increase in the amount of steel in the cores in the M1 was not optimal, since when comparing the ductility in both walls, the M1 presents less ductility because there is more steel in the traction zone.

Keywords Cutting walls · Moment curvature · Axial load · Numerical analysis

M. D. H. Martel (✉) · J. J. C. Taipe · J. A. C. Gonzalez · J. J. H. Yucra
School of Civil Engineering, Universidad Continental, Huancayo, Perú
e-mail: 73331527@continental.edu.pe

J. J. C. Taipe
e-mail: 73991701@continental.edu.pe

J. A. C. Gonzalez
e-mail: 75388855@continental.edu.pe

J. J. H. Yucra
e-mail: jhinostrozay@continental.edu.pe

M. Casini (ed.), *Proceedings of the 3rd International Civil Engineering and Architecture Conference*, Lecture Notes in Civil Engineering 389,
https://doi.org/10.1007/978-981-99-6368-3_22

1 Introduction

The shear walls have been used especially in high-rise buildings to resist seismic loads [1]. These walls are critical in seismically active areas since there is an increase in shear force in the structure [2]. Which are designed to have a no-linear behavior in severe seismic, where the input seismic energy is absorbed [3].

Likewise, the design of shear walls requires to estimate of their load capacity as well as their resistance for lateral displacement; in addition, the seismic events raised have highlighted their seismic performance [4]. However, pre-existing buildings show that shear walls lack some ductility [5]. One of the most appropriate options for concrete structures against seismic loads is to increase their ductility [6]. Due to this, it is necessary to simulate its behavior with greater precision, where the curvature moment relationship of concrete elements is considered as well as the stress-deformation relationship of confined and unconfined concrete [7].

Studies of shear walls have been observed in which the curvature moment decreased when the axial loads increased, resulting in the concrete´s immediate deformation. Likewise, parameters such as material properties, amount of reinforcement and geometry of the section influence the calculation of the curvature moment diagram [8].

2 Methodology

In this study, the “C” shaped reinforced concrete walls M1 and M2 were analyzed with variability in the longitudinal reinforced of the cores. With the intention of comparing the ductility of both walls with a variation of axial loads from 980.6 to 7844.8 KN, also evaluating the ductility in relation to the change of longitudinal reinforced in the cores. With a positive “y” eccentricity. Considering f’c 2059.4 N/cm^2 and the perfect elastoplastic model of steel with fy 41,187.93 N/cm^2.

3 Construction of the Curvature Moment Diagram

The models of idealization of curvature moment allow validating the behavior of the wall, therefore, in the present study the proposed model from the Book of Eng. Ottazzi was used, which details the cracking point of the concrete and limits the yield point that requires variability of the stiffness of the section in study [10]. (See Fig. 1).

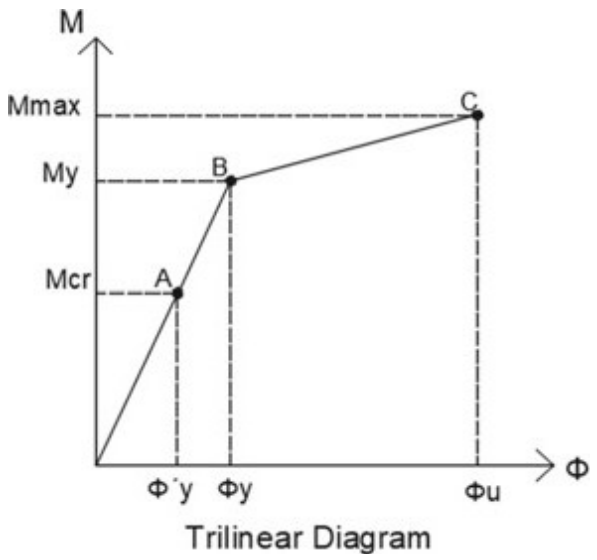

Fig. 1 Curvature Moment Diagram. Adapted of "Apuntes del Curso de Concreto Armado 1" [10]

3.1 Hypothesis to Consider Generating the Moment–Curvature Diagram

The following points were taken into consideration for the numerical analysis proposed by the research: The section under analysis is flat and remains flat. There is no early failure by cutting, or by lateral buckling. The bending tensile strength of concrete can be estimated as $2\sqrt{\mathbf{f'c}}\left(\frac{\text{kgf}}{\text{cm}^2}\right)$. There is a perfect adhesion between concrete and steel [10].

3.2 Cracking Point (Point A—Mcr)

The point at which the section under analysis reaches the maximum tensile strength of the concrete, thus initiating the cracking of the concrete. After this point, the cracked area of the concrete was neglected in the numerical analysis, so the only one that provides tensile strength is steel [10]. When comparing the moment of cracking and the last moment of a wall this is significantly greater than the moment of cracking which demonstrates low plasticity or seen otherwise allows very little inelastic deformation [11]. Minimal reinforcement in concrete walls can increase the cracking moment up to 1.5 times its value [11].

3.3 Creep Point (Point B—My)

Steel creep starting point, the unit deformation of the steel reaches $\varepsilon y = 0.0021(0.21\%)$. One of the most representative states of a moment–curvature diagram, which precedes the failure point of the section and in turn represents the end of elastic behavior, relating the yield moment (My) and the creep curvature (φy) [10].

To appreciate the behavior of the concrete wall depends on variables such as the form of application of loads, and the relationship between steel and concrete, which is the reason for the existence of several constitutive laws, therefore, we worked with the constitutive law of Hognestad that represents the model of stress deformation related to maximum effort and with a deformation of exhaustion of εo = 0.002 [9]. "Eq. (1) and (2)" defines Hognestad's proposed constitutive law.

$$fc = f''c*\left[\frac{2\varepsilon c}{\varepsilon 0} - \left(\frac{\varepsilon c}{\varepsilon o}\right)^2\right]\left(\frac{\text{kgf}}{\text{cm}^2}\right);\ 0 \le \varepsilon c \le 0.002 \tag{1}$$

where:

$$\varepsilon_0 = \frac{2*f''c}{Ec} \tag{2}$$

When performing tests on columns placed vertically with eccentric loads, an average value of maximum bending stress, f", which is equal to 0.85f'c (kgf/cm^2) [9] was found.

Point of Depletion (Point C—Mmax). After exceeding the admissible stresses, the section does not fail, it still has a reserve that is used in the design for resistance which we call a point of exhaustion or maximum capacity. The ACI and Peruvian regulations accept the simplification of an equivalent block of compressions or Whitney rectangle [10].

3.4 Ductility

Ductility is the property that allows deforming the plastic state without reaching the fault. Consequently, the ductility of curvature is the ratio of the curvature of the concrete at its point of exhaustion, which means the concrete has reached a deformation Ec = 0.003 without any steel failing by breakage and the first creep of the steel to tension [10]. Ductility is the ability of a material or structure under inelastic conditions to withstand loads [12]. During an earthquake, the energy is absorbed by the structure which will be dissipated by the plastic deformation of the components [13]. "Eq. (3) defines the ductility of the section under analysis".

$$\mu\varphi = \frac{\varphi max}{\varphi y} \tag{3}$$

4 Results

The following figures show the reinforcements used in the M1 and M2 walls (see Figs. 2 and 3).

The following table shows the summary of the values calculated at each point of the Moment—curvature of the M1 Diagram (see Table 1).

The following figure shows the moment–curvature diagram as a function of the variation of the axial load on wall M1 (see Fig. 4).

The following table shows the summary of the values calculated at each point of the Moment—curvature of the M2 Diagram (see Table 2).

The following figure shows the moment–curvature diagram as a function of the variation of the axial load on wall M2 (see Fig. 5).

The following tables summarize the ductility calculations in walls M1 and M2 as a function of the variation of the axial load (see Tables 3 and 4).

The following figure shows the comparison of ductility in walls M1 and M2 as a function of axial load variation (see Fig. 6).

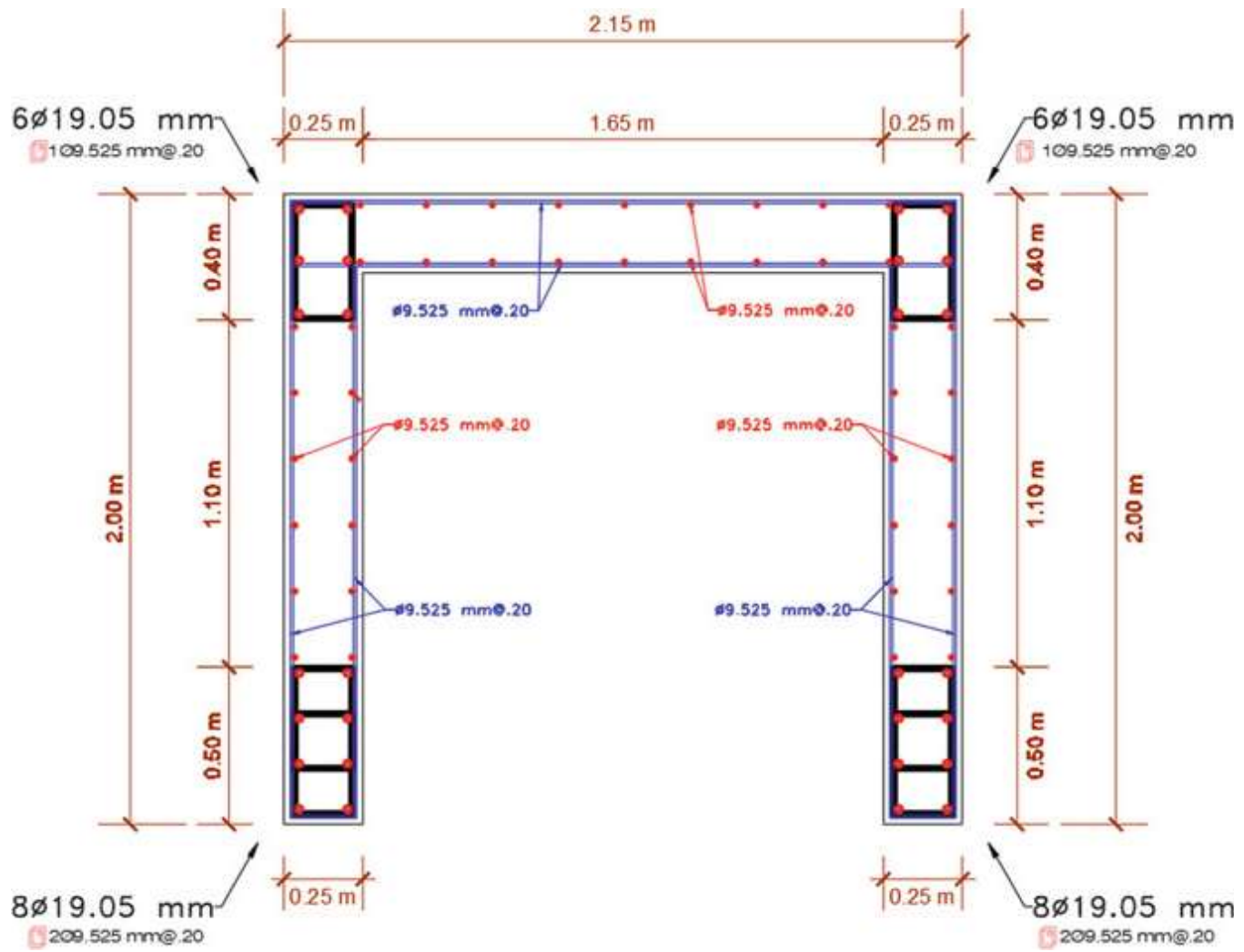

Fig. 2 M1 reinforcement proposal 1

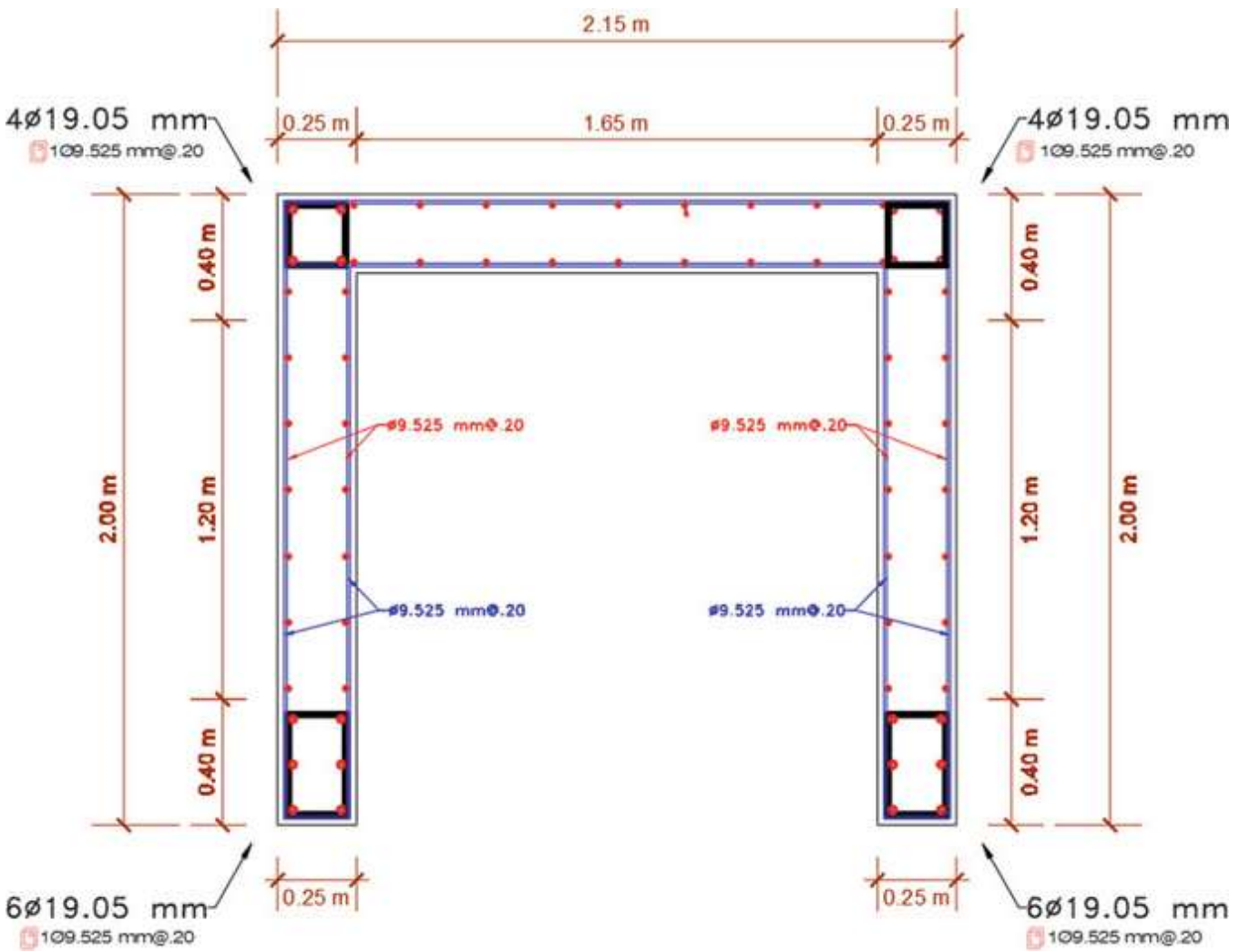

Fig. 3 M2 reinforcement proposal 2

Table 1 Result of generating the moment—curvature diagram with axial load variation of wall 1 Type C

Wall 1 Type C						
Axial load	Concrete cracking point		Steel creep point		Point of failure o maximum capacity	
	M cr	φ	My	φy	M max	φmax
KN	KN m	$10^{-3}\ \frac{1}{m}$	KN m	$10^{-3}\ \frac{1}{m}$	KN m	$10^{-3}\ \frac{1}{m}$
980.6	1716.05	0.25	4095.38	1.32	5141.38	23.59
1961.2	2036.80	0.33	5114.71	1.38	6169.74	20.23
3922.4	2678.31	0.49	7114.74	1.51	8186.83	15.23
5883.6	3319.76	0.65	9063.59	1.64	10,114.30	12.11
7844.8	3961.23	0.81	10,961.74	1.77	11,950.33	9.88

5 Discussion of Results

When performing an analysis of the formulas used and the results obtained in the research it was observed that the parameter “c” represents the distance or compressed area in the direction in which the analysis was performed, when increasing its value

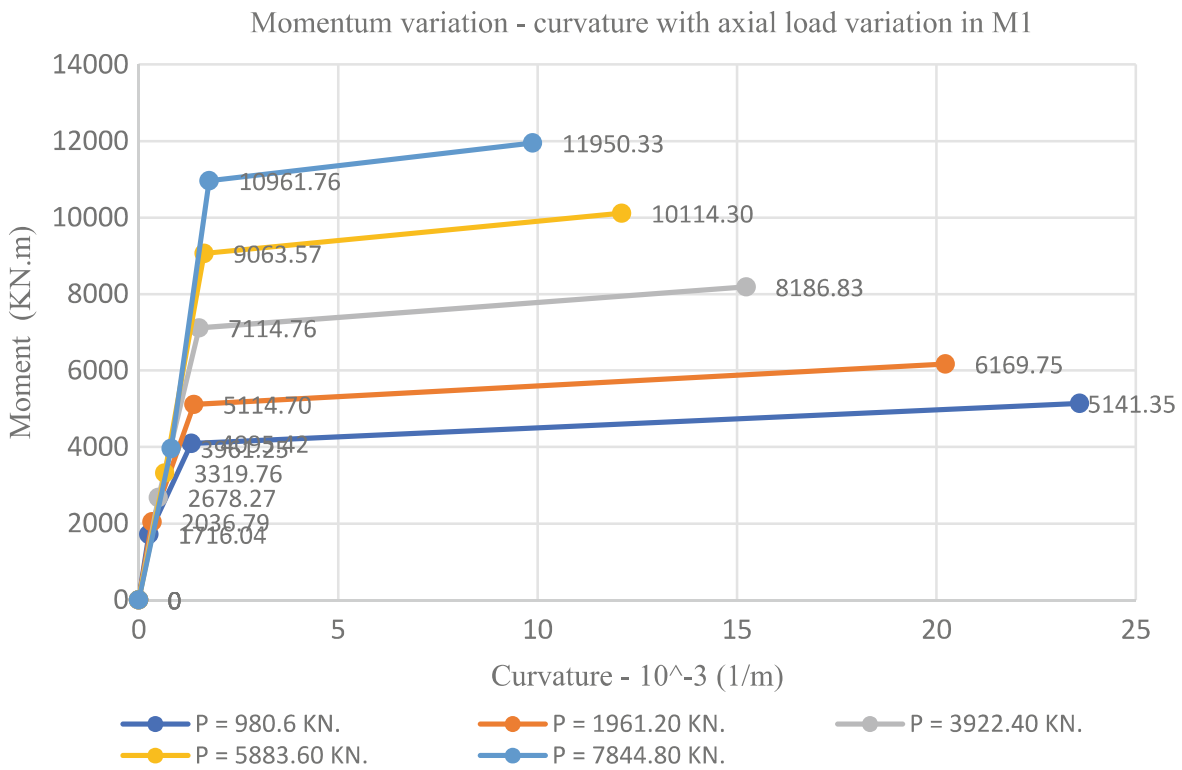

Fig. 4 Result of generating the moment—curvature with axial load variation of the M1 type C

Table 2 Result of generating the moment—curvature diagram with axial load variation of M2 Type C

Wall 2 type C						
Axial load	Concrete cracking point		Steel Creep Point		Point of failure o maximum capacity	
	M cr	φ	My	φy	M max	φmax
KN	KN m	$10^{-3}\ \frac{1}{m}$	KN m	$10^{-3}\ \frac{1}{m}$	KN m	$10^{-3}\ \frac{1}{m}$
980.6	1700.93	0.26	3683.23	1.30	4441.94	28.36
1961.2	2021.64	0.34	4720.07	1.37	5500.34	22.98
3922.4	2663.07	0.50	6752.58	1.50	7542.79	17.08
5883.6	3304.49	0.66	8731.02	1.63	9514.16	13.25
7844.8	3945.92	0.82	10,656.90	1.76	11,413.58	10.69

this inversely influences the curvature, in the same way to ductility; In other words, if the compressed area is larger the ductility will be lower. To increase the ductility in any section you have to reduce the value of this parameter, for which you had to increase the amount of steel in the compressed area and increase the f'c, another option was to increase the width of the compressed area.

The proposal to place more steel in the compressed area is not possible in all cases since many of the structural elements in which they act forces in flexion or flexo-compression, these forces act in different directions, which can vary the compressed area making the steel that was placed to decrease the parameter "c" in that direction of analysis, It can be more detrimental in a reverse direction since the parameter "C" depends not only on the width of the compressed zone and the steels in it, but

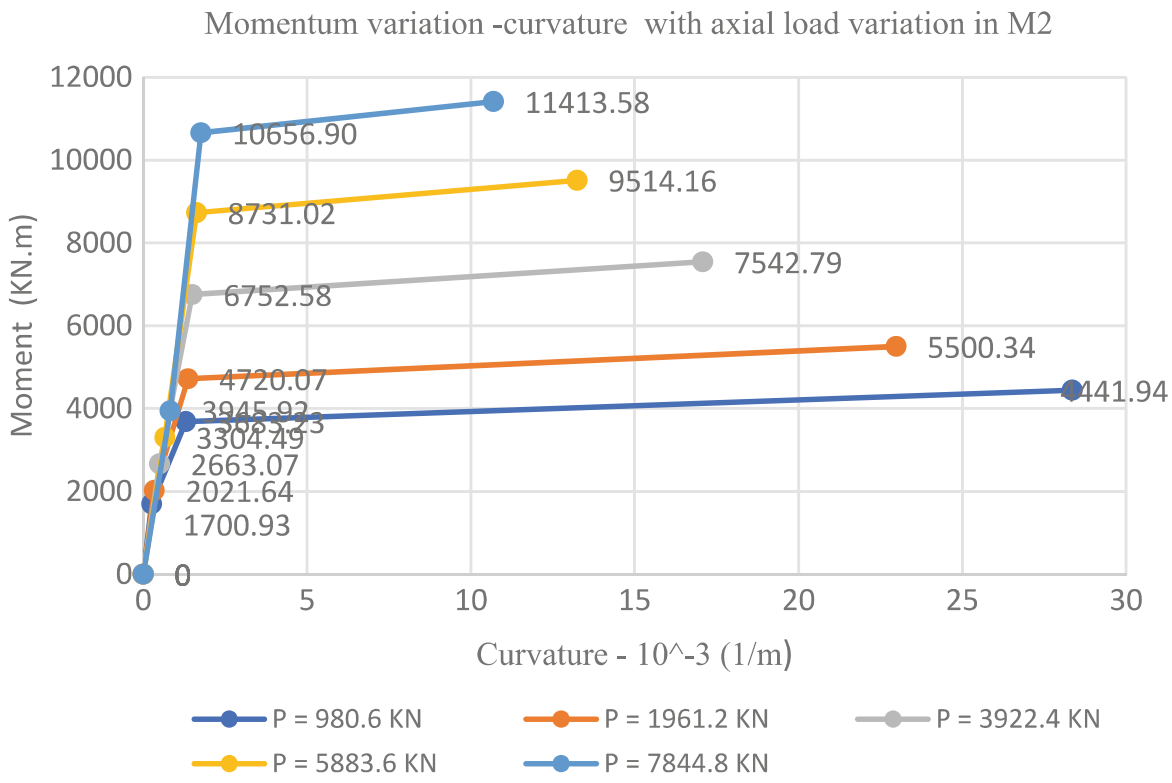

Fig. 5 Result of generating the moment—curvature diagram with axial load variation of wall 2 type C

Table 3 Axial load versus wall ductility 1 Type C

Axial load (KN)	Ductility
980.6	17.88
1961.2	14.61
3922.4	10.08
5883.6	7.39
7844.8	5.58

Table 4 Axial load versus wall ductility 2 Type C

Axial load (KN)	Ductility
980.6	21.85
1961.2	16.83
3922.4	11.42
5883.6	8.15
7844.8	6.08

also the steels that are in the tensile zone. Seen another way if there is more steel in the traction zone, the parameter "c" must have a higher value to balance the internal forces in the section.

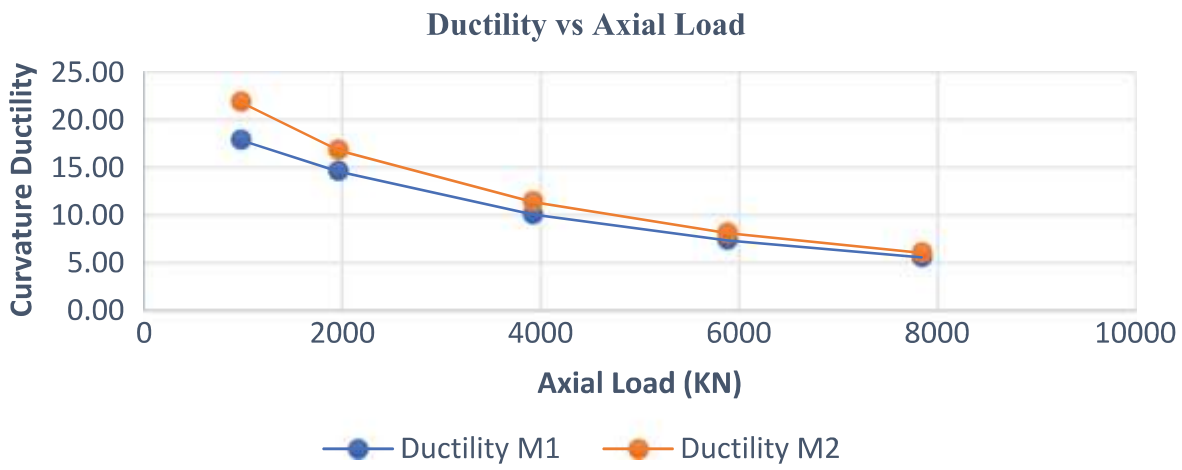

Fig. 6 Comparison of the ductility of both diagrams moment—curvature with respect to the variation of the axial load

6 Conclusion

To sum up, the axial load significantly influences each point of the Moment – Curvature diagram, since in both analyzes as the axial load increases it is necessary to apply a greater moment to reach the cracking points of the section (Mcr), the yield point of the steel (My) and point of exhaustion or maximum capacity (Mmax).

(1) In M1 and M2 the (Mcr) with axial load of 980.6 KN. is 1716.04 KN.m and 1700.93 KN.m for axial loads of 1961.2, 3922.4, 5883.6, 7844.8 KN the value of (Mcr) for M1 increases by 18.69%, 56.07%, 93.45% 130.84% respectively and for M2 the increase is 18.86%, 56.57%, 94.28% 131.99% respectively.
(2) In M1 and M2 the (My) with axial load of 980.6 KN. is 4095.42 KN.m and 3683.23 KN.m, for the axial loads of 1961.2, 3922.4, 5883.6, 7844.8 KN. the value of (My) for the first wall increases by 24.89%, 73.72%, 121.31% 167.66% respectively and for the second wall the increase is 28.15%, 83.33%, 137.05% 189.34% respectively.
(3) In M1 and M2 the (Mmax) with axial load of 980.6 KN. is 5141.35 KN.m and 4441.94 KN.m, for the axial loads of 1961.2, 3922.4, 5883.6, 7844.8 KN. the value of (Mmax) for the first wall is increased by 20%, 59.23%, 96.72% 132.44% respectively and for the second wall the increase is 23.83%, 69.81%, 114.19% 156.95% respectively.
(4) It can also be observed that the greater the axial load, the cracking points (Mcr), and the steel yield point (My) have greater curvature as the axial load increases.

If the diagrams of both walls in the analysis are compared with the same axial load, the wall with less longitudinal reinforcement in the cores requires a lower moment value to bring to each point of the diagram, but the curvature at the points of cracking of the section and of exhaustion or maximum capacity is greater except for the yield point at which the wall with the greatest reinforcement in the cores has a greater curvature.

When increasing the value of the axial load the ductility of the wall decreases, since, for an axial load of 980.6 KN the ductility of the first and second wall is 17.88

and 21.85, for the axial loads of 1961.2, 3922.4, 5883.6, 7844.8 KN the ductility in the first wall decreases by 18.28, 43.63, 58.64, 68.77% and in the second wall decreases by 22.96, 47.73, 62.70 and 72.19%.

Finally, the way in which the amount of steel in the core was increased was not optimal, since it did not help greatly to increase the ductility of wall 1, and even this was more harmful. Thanks to the analysis of formulas used and results, it was concluded that it is necessary to increase the steel in the cores in such a way that, when performing the analysis in opposite directions, the wall presents a balanced ductility in both directions.

References

1. Marzok A, Lavan O, Dancygier AN (2020) Predictions of moment and deflection capacities of RC shear walls by different analytical models. In: Structures. Elsevier, pp 105–127. https://doi.org/10.1016/j.istruc.2020.03.059
2. Fadallah R et al (2022) Experimental investigation of small-scale shear walls under lateral loads. J Eng Appl Sci 2022 69(1):1–19. https://doi.org/10.1186/s44147-022-00141-0
3. Gu A et al (2019) Experimental study and parameter analysis on the seismic performance of self-centering hybrid reinforced concrete shear walls. Soil Dyn Earthq Eng 116:409–420. https://doi.org/10.1016/j.soildyn.2018.10.003
4. Mangalathu, S et al (2020) Data-driven machine-learning-based seismic failure mode identification of reinforced concrete shear walls. Eng Struct 208:110331. https://doi.org/10.1016/j.engstruct.2020.110331
5. Paulay T (1975) Design aspects of shear walls for seismic areas. Can J Civ Eng 2(3):321–344. https://doi.org/10.1139/l75-030
6. Mohemmi M (2022) An algorithm to obtain moment-curvature diagram for reinforced concrete sections. In: International conference on civil engineering. Springer, Singapore, pp 31–45. https://doi.org/10.1007/978-981-19-1260-3_4
7. Foroughi S, Yüksel B (2020) Investigation of nonlinear behavior of high ductility reinforced concrete shear walls. Int Adv Res Eng J 4(2):116–128. https://doi.org/10.35860/iarej.693724
8. Wang B, Cai W, Shi Q (2019) Simplified data-driven model for the moment curvature of T-shaped RC shear walls. Adv Civ Eng 2019. https://doi.org/10.1155/2019/9897827
9. Hognestad E (1951) Study of combined bending and axial load in reinforced concrete members. University of Illinois at Urbana Champaign, College of Engineering. Engineering Experiment Station
10. Ottazzi G (2016) Apuntes del curso Concreto Armado 1. 15ava edición. Lima-Perú Pontificia Universidad Católica del Perú
11. Hoult R, Goldsworthy H, Lumantarna E (2018) Plastic hinge length for lightly reinforced rectangular concrete walls. J Earthq Eng 22(8):1447–1478. https://doi.org/10.1080/13632469.2017.1286619
12. Nurjannah S et al (2023) The analysis of numerical self-compacting concrete wall panel models with variations of shear reinforcement. Eng Solid Mech 11(1):89–102. https://doi.org/10.5267/j.esm.2022.8.002
13. Zhang L et al (2022) Experimental study on the seismic behavior of squat SRC shear walls with high axial load ratio. Buildings 12(8):1238. https://doi.org/10.3390/buildings12081238